Physica C 468 (2008) 1032–1035

Contents lists available at ScienceDirect

Physica C

journal homepage: www.elsevier.com/locate/physc

Effects of TiC doping on the upper critical field of MgB_2 superconductors

S.C. Yan [a,b,*], L. Zhou [a,b], G. Yan [b], Y.F. Lu [b]

[a] School of Materials Science and Engineering, Northwestern Polytechnical University, Xi'an, Shaanxi 710072, PR China
[b] Northwest Institute for Nonferrous Metal Research, P.O. Box 51, Xi'an 710016, PR China

ARTICLE INFO

Article history:
Received 2 March 2008
Received in revised form 28 April 2008
Accepted 8 May 2008
Available online 20 May 2008

PACS:
74.72.Yg

Keywords:
MgB_2
TiC doping
Upper critical field
Two-step reaction method

ABSTRACT

TiC doped MgB_2 bulks were fabricated by two-step reaction method. The sample with a nominal compositions of $Mg(B_{0.95}(TiC)_{0.05})_4$ was first sintered at 1000 °C for 0.5 h. An appropriate amount of Mg was added to reach the stoichiometry of $Mg(B_{0.95}(TiC)_{0.05})_2$, which was sintered at 750 °C for 2 h.
The H_{c2} for the micro-TiC doped MgB_2 reached 12 T at 20 K. And J_c is 5.3×10^4 A/cm^2 at 20 K and 1 T. The results indicate that the two-step reaction method could effectively introduce the carbon in TiC into the MgB_2 crystalline lattice, and therefore improve the upper critical field.

1. Introduction

The enhancement of upper critical field (H_{c2}) for MgB_2 superconductors is crucial for magnet applications. The better results to improve the H_{c2} of MgB_2 are achieved in the carbon [1–5] or carbides [6–8] doped MgB_2. Since carbon has one more electron than boron, it is expected that electrons are doped into the system by carbon substitution. The increase of H_{c2} for the carbon doped MgB_2 is attributed to its two-gap nature. An earlier work has shown that in C-doped MgB_2 thin films the H_{c2} (0 K) can exceed 70 T [5]. However, for C or SiC doped wires or bulks the H_{c2} (0 K) is close to 35–40 T [3,8]. The carbon solubility in MgB_2 varies considerably depending on the synthesis route and starting materials. Mickelson et al. [8] achieved better mixing of B and C atoms using boron carbides B_4C as a source of carbon. The samples had an estimated composition $Mg(B_{0.9}C_{0.1})_2$. Ribeiro et al. [9] reported that the carbon substitution level is about 10% in the nearly single-phase $Mg(B_{1-x}C_x)_2$ sample, it is most likely solid solubility of carbon in polycrystalline MgB_2 obtained under ambient pressure. Recently, Kazakov et al. [3] found that the carbon solubility can reach to 15% in the carbon doped single crystal MgB_2 sample obtained under high pressure. However, the highest H_{c2} in carbon doped MgB_2 sample can be achieved by the carbon substitution around 3–5% per boron atom [3,8]. In general, the MgB_2 samples were prepared by sintering the mixed powders of Mg, B and dopants in previous experiments. The so-obtained polycrystalline MgB_2 samples have a high porosity, which is a limit for promoting the increase of current density of MgB_2 superconductors due to decreasing the effective carried current area. In addition, the nano-scale dopants were widely used in order to improve the reactivity of dopants. This causes the material costs to increase substantially due to the higher price for the nano-scale doping powders. To solve above problems we have developed the two-step reaction method. This method is used to fabricate the lower cost micro-scale C [10] and SiC [11] doped MgB_2 bulks. The experimental results clearly demonstrate that this method could effectively increase both the sample density and reactivity of micro-scale dopants, and therefore improve the superconducting performance of MgB_2.

In this work, we have investigated the doping effect of TiC on the superconducting properties of MgB_2. The nano-TiC and the micro-TiC doped MgB_2 bulks were obtained by single step reaction and two-step reaction methods, respectively. It is found that the H_{c2} of the TiC doped MgB_2 obtained by two-step reaction are improved significantly.

2. Experiments

Using the powders of magnesium (99%, −325mesh), amorphous boron (99.9%, 1–2 μm), and TiC (99.9%, <5 μm) as raw materials,

* Corresponding author. Address: School of Materials Science and Engineering, Northwestern Polytechnical University, Xi'an, Shaanxi 710072, PR China. Tel.: +86 29 86231079; fax: +86 29 86224487.
E-mail address: yscfei@tom.com (S.C. Yan).

0921-4534/$ - see front matter © 2008 Elsevier B.V. All rights reserved.
doi:10.1016/j.physc.2008.05.003

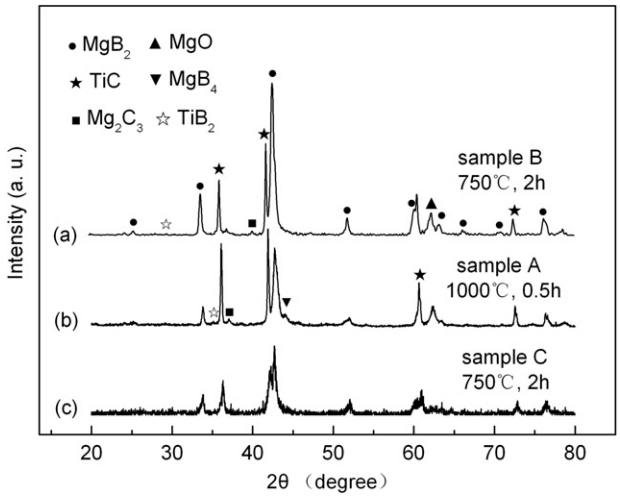

Fig. 1. XRD patterns for the sample A, B and C.

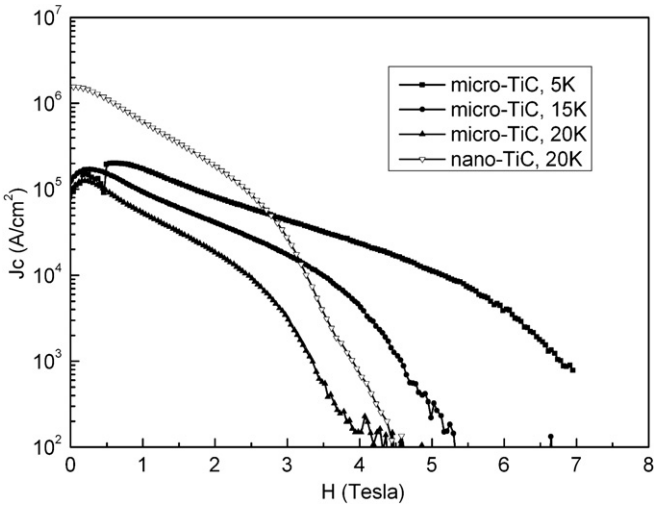

Fig. 2. Critical current density at various field and temperatures using Bean's model for the sample B and C.

the bulk $Mg(B_{0.95}(TiC)_{0.05})_2$ samples were prepared by two-step reaction method. In the first step, in order to decrease the Mg volatilization these powders were mixed with the stoichiometry of $Mg(B_{0.95}(TiC)_{0.05})_4$ (sample A) by mechanical grinding, and then pressed into pellet with the dimension of $\Phi 2 \times 0.5$ cm under a pressure of 10 MPa. The pellet was put into a niobium crucible, then heat treated in high purity Ar with the heating rate of 20 °C/min starting from room temperature and followed to room temperature by a furnace cooling. The higher sintering temperature of 1000 °C for 0.5 h is selected due to the carbon in TiC easily substitutes the boron. In the second step, the sample A was ground into powders by mechanical grinding. An appropriate amount of Mg powder was mixed with the ground powders for reaching to the stoichiometry of $Mg(B_{0.95}(TiC)_{0.05})_2$ (sample B), which was heat treated at 750 °C for 2 h. In addition, a reference sample $Mg(B_{0.95}(TiC)_{0.05})_2$ (sample C) with nano-TiC (99.9%, 40 nm) was synthesized by single step reaction at 750 °C for 2 h.

MgB_2 bulk samples were characterized by the X-ray diffraction (XRD) for phase identification on the Philips APD 1700 diffractometer, scanning electron microscope (SEM) of JSM6460 for microstructural observation, and by dispersive X-ray spectroscopy (EDS) for element mappings. Bar shaped sample with a dimension of about $a \times b \times c = 1.3 \times 1.3 \times 0.7$ mm^3 was cut from as sintered pellets for magnetic measurements. The magnetization was measured over a wide temperature range between 5 and 20 K in 0–9 T using a Quantum Design PPMS. The magnetic J_c was calculated from the width of hysteresis loop (M–H) using a Bean model where $J_c = 20\ \Delta M/[a(1 - a/3b)]$, where a and b are the dimensions of the sample perpendicular to the direction of applied field. The resistivity transitions in fields up to 12 T were measured by standard four-probe method.

3. Results and discussion

Fig. 1 shows the XRD patterns for the sample A, B and C. It can be seen that for the sample A the MgB_2 is a major phase, and small amount of MgB_4, TiB_2 and Mg_2C_3 are formed. This indicates that the reaction of $3Mg + 3TiC + 8B = MgB_2 + 3TiB_2 + Mg_2C_3$ take places in the first step sintering reaction. Indeed, as reported by

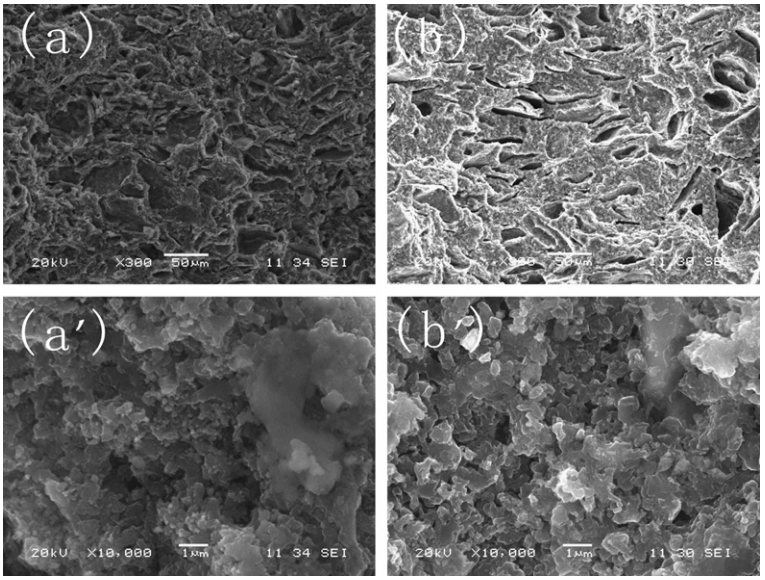

Fig. 3. The typical SEM images for the sample C (a, a') and B (b, b').

Yamamoto et al. [12] that the reaction between micro-TiC and Mg could occur when the sintering temperature is higher than 950 °C. The MgB_4 are resulted from the decomposition of MgB_2 [13]. For the sample B, we can see that the MgB_4 phase fully disappears. This is because the reaction between MgB_4 and Mg to form MgB_2 occurs during the second sintering step. Furthermore, in this sintering stage the reaction of Mg and excess B to form MgB_2 will occur, and the new formed MgB_2 grains and others formed at the first sintering step connect each other.

It was demonstrated that the *a*-axis lattice parameters of MgB_2 decreases with increasing the amount of carbon incorporated into the lattice [3]. In our case, the lattice parameters of sample A, B and C respectively are $a = 3.079$, $c = 3.525$, $a = 3.076$, $c = 3.524$ and $a = 3.081$, $c = 3.525$ calculated by using Powder X program [14]. The *a*-axis lattice parameters of sample B is clearly lower than that of sample A and C, indicating that the two-step reaction method is favorable for the carbon substitution of B sites in the TiC doped MgB_2.

Fig. 2 shows J_c(H,T) for the sample B and C as a function of the magnetic field at 5 K, 15 K and 20 K. It can be seen that at 20 K the J_c of sample C is higher than that of sample B in available magnetic field, for the sample C and B the value of J_c at 20 K and 2 T are 2×10^5 A/cm^2 and 1.8×10^4 A/cm^2, respectively. The typical SEM images for the sample C and B are presented in Fig. 3a and b, respectively. It can be seen that the micro-scale pore formed in the sample B due to the vacancy and evaporation of magnesium [15]. The porosity of sample C is evidently lower than that of sample B, which probably is attributed to that the nano-TiC particles is beneficial for the denseness of MgB_2 sample. On the other hand, apparently the average grain size of sample C (see Fig. 3a') is smaller than in the case of sample B (see Fig. 3b'). The backscatter image of sample C is shown in Fig. 4. Apparently, the nano-TiC particles distribute uniformly in the MgB_2 matrixes, which could restrain the growth of MgB_2 grain, therefore the grain size in sample C is small compared to that in sample B. It should be pointed out that for the sample C the fine MgB_2 grain is beneficial for enhancing the flux pinning ability due to increase of grain boundary density. For the sample B, the elemental mapping was also carried out in the present area (see Fig. 5). The EDS maps show that the big grains of un-reacted TiC can be easily seen in the MgB_2 matrix, which is in agreement with its XRD pattern. The un-reacted micro-TiC particles probably bring weak links at grain boundaries and therefore decrease the J_c of sample B. It notes that the drop of J_c of sample C with increasing the magnetic field is clearly faster than that of sample B when the magnetic field is higher than 2 T. This indicates that the flux pinning ability under high magnetic fields is enhanced in the sample B, probably due to the higher carbon substitute level in the sample B if compared with the sample C. In other words, this mean that the big micro-scale TiC particles in the sample B lead to the weak flux pinning ability and therefore decrease the J_c under low magnetic fields, the strong flux pinning ability under high magnetic fields is resulted from the improving reactivity of micro-TiC due to the sample B obtained by using the two-step reaction method.

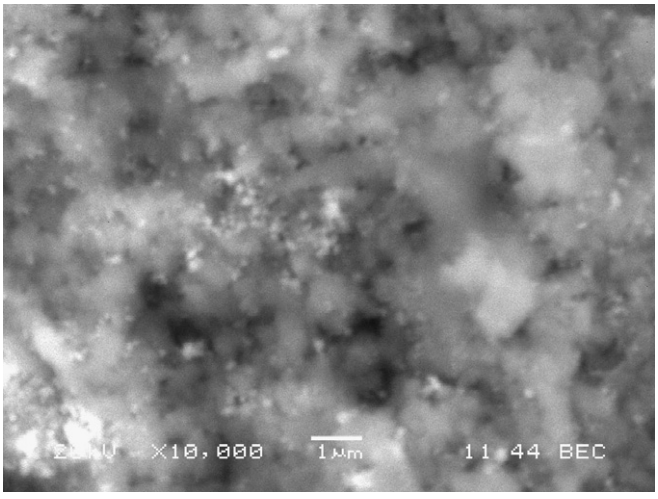

Fig. 4. The backscatter image for the sample C.

Superconducting transition curves were measured by a conventional four-probe resistive method in magnetic fields up to 12 T with an applied DC current of 20 mA. The values of T_c^{onset} for the sample B and C were determined from the ρ–T curves at 0 T, which are 37.8 K and 38.3 K, respectively. H_{irr} and H_{c2} of sample B and C are shown in Fig. 6, which obtained from the resistive transition curves (here, the pictures is not shown), where 10% and 90% tran-

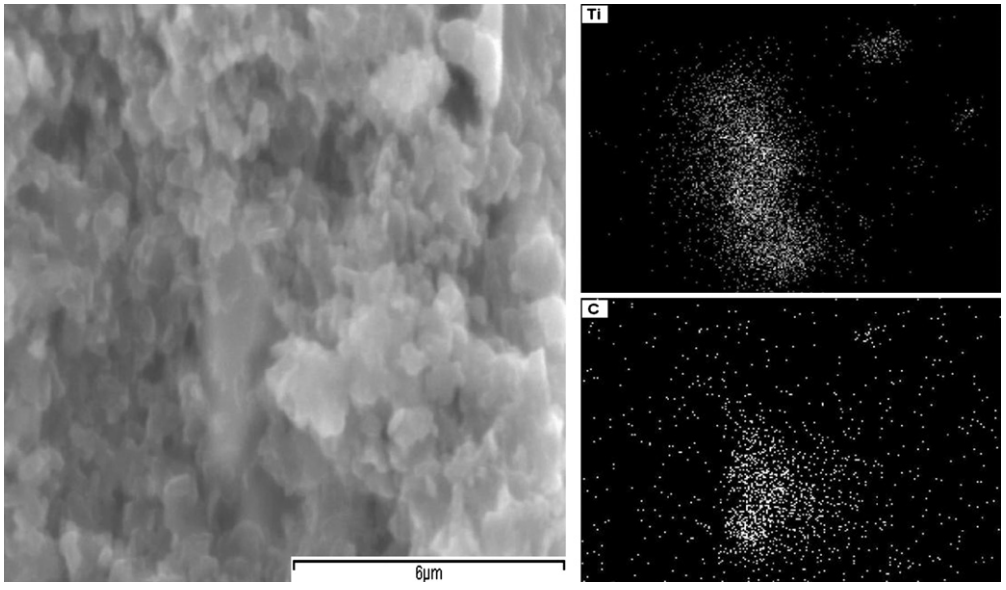

Fig. 5. The EDS map for the sample B.

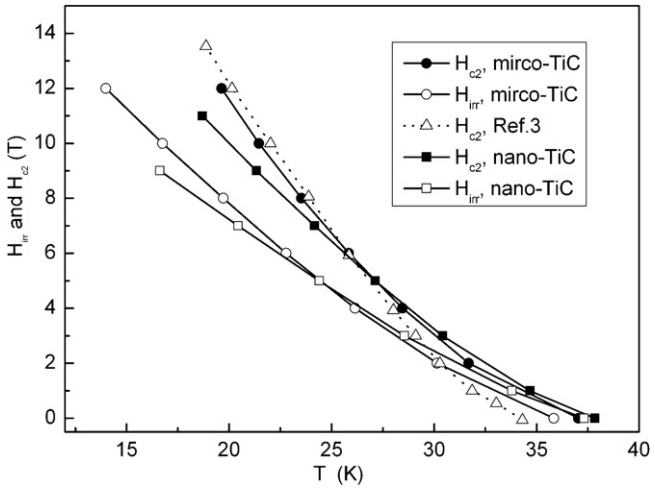

Fig. 6. Temperature dependence of the irreversibility field H_{irr} and upper critical field H_{c2} for the sample B and C.

sition points on the resistive transition can be taken to approximate H_{irr} and H_{c2} for the field parallel to the boron and magnesium planes. The value of H_{c2} for nano-C doped MgB_2 single crystal (Ref. [3]) also is shown in Fig. 6 for comparison. We can see that the H_{c2} and H_{irr} of sample C are lower than that of sample B, the H_{c2} of sample B is much close to that of nano-C doped MgB_2 single crystal. For example, at 20 K, the values of H_{c2} for aforementioned three samples are 10 T, 12 T and 12.4 T, respectively. Apparently, our results indicate that the two-step reaction is beneficial for improving the superconducting properties of MgB_2.

4. Summary

In summary we have investigated the doping effects of TiC on the superconducting properties of MgB_2 superconductors. The nano-TiC and micro-TiC doped MgB_2 bulks were prepared by single step reaction and two-step reaction, respectively. The SEM results indicated that the grain size of MgB_2 in nano-TiC doped sample is smaller than that of micro-TiC doped sample. Improved J_c properties were observed for the nano-TiC doped MgB_2 due to increase of grain boundaries. The XRD results indicated that the two-step reaction method could increase the reactivity of micro-TiC, therefore effectively incorporate the carbon in TiC into the lattice of MgB_2. The micro-TiC doped MgB_2 prepared by two-step reaction can produce H_{c2} much close to that obtained for carbon doped MgB_2 single crystal, for example 12 T at 20 K.

Acknowledgments

This work is supported by the National Natural Science Foundation of China under the Contract No. 50472099, the National Basic Research Program of China under the Contract No. 2006CB601004 and the Doctorate Foundation of Northwestern Polytechnical University of China.

References

[1] B.J. Senkowicz, J.E. Giencke, S. Patnaik, et al., Appl. Phys. Lett. 86 (2005) 202502.
[2] H.T. Wilke, S.L. Bud'ko, P.C. Canfield, et al., Physica C 424 (2005) 1.
[3] S.M. Kazakov, R. Puzniak, K. Rogacki, et al., Phys. Rev. B 71 (2005) 024533.
[4] S. Lee, T. Masui, A. Yamamoto, H. Uchiyama, et al., Physica C 397 (2003) 7.
[5] C.B. Eom, M.K. Lee, J.H. Choi, et al., Nature 411 (2001) 558.
[6] W. Mickelson, J. Cumings, W.Q. Han, et al., Phys. Rev. B 65 (2002) 052505.
[7] S. Soltanian, X. Wang, J. Horvat, et al., Supercond. Sci. Technol. 18 (2005) 658.
[8] A. Matsumoto, H. Kumakur, H. Kitaguchi, et al., Appl. Phys. Lett. 89 (2006) 132508.
[9] R.A. Ribeiro, S.L. Bud'ko, C. Petrovic, et al., Physica C 384 (2003) 227.
[10] S.C. Yan, G. Yan, L. Zhou, et al., Supercond. Sci. Technol. 20 (2007) 377.
[11] S.C. Yan, G. Yan, Y.F. Lu, et al., Supercond. Sci. Technol. 20 (2007) 549.
[12] A. Yamamoto, J. Shimoyama, S. Ueda, et al., Physica C 445–448 (2006) 801.
[13] S.C. Yan, L. Zhou, G. Yan, et al., J. Am. Ceram. Soc. 90 (2007) 2184.
[14] C. Dong, J. Appl. Cryst. 32 (1999) 838.
[15] S.C. Yan, G. Yan, C.F. Liu, et al., J. Alloy Compd. 437 (2007) 298.